Photoacid Generators for Catalytic Decomposition of Polycarbonate

Mark G. Cupta, Paul Jayachandran Joseph, Paul A. Kohl

School of Chemical and Biomolecular Engineering, Georgia Institute of Technology, Atlanta, Georgia 30332-0100

Received 4 April 2006; accepted 15 February 2007
DOI 10.1002/app.26343
Published online 11 May 2007 in Wiley InterScience (www.interscience.wiley.com).

ABSTRACT: The photo-activated, acid catalyzed decomposition of polycarbonate was investigated in this study. The impact of the chemical and physical properties of the photoacid generators (PAG) and the ambient atmosphere effect on polycarbonate decomposition were discussed. The photo-patterns resulted from the photoacid catalyzed decomposition of a polycarbonate can be used as a sacrificial placeholder for fabrication of microelectromechanical and microfluidic devices. The effects of acid strength, vapor pressure of the acid, PAG activation process, and ambient conditions (temperature, moisture, and oxygen concentrations) on polymer film decomposition were studied. Several superacids (e.g. triflic and nonaflic based PAGs) were not suitable for decomposition of the polycarbonate because of their high vapor pressures resulting in the high volatility properties. From the decomposition experiments it was found that the nonfluorinated sulfonic acid based PAGs do not posses the superacidity needed for decomposition. Perfluorinated methide and a tetrakis (pentafluoropheyl)borate PAG were effective in the decomposition of polycarbonate films. The combination of two PAGs, one which generates high vapor pressure acid (thus, highly volatile) and the other with a lower vapor pressure acid (thus, less volatile) showed very low residue levels. This is because of the volatility of the generated high vapor pressure acid (usually remaining acid in the film was the cause of the residue left behind) and the remaining nonvolatile low vapor pressure acid was sufficient to decompose the polycarbonate that was not decomposed by the generated high volatile acid. © 2007 Wiley Periodicals, Inc. J Appl Polym Sci 105: 2655–2662, 2007

Key words: polycarbonates; photochemistry

INTRODUCTION

Polymer systems with low decomposition temperatures used as sacrificial placeholders polymers in the fabrication of a variety of microelectromechanical (MEMS) and microfluidic applications.[1–5] Sacrificial polymers serve as temporary material that was thermally released in the fabrication process. After patterning the sacrificial polymer and overcoating it with a second dielectric material, the polymer can be converted into a gas upon thermal heating, which permeates through the overcoat polymer during sacrificial polymer decomposition. The resulting air-cavity can be used in the packaging of MEMS devices like gyroscopes and micromechanical resonators.[6,7] Additionally, they are used to form systems of microchannels to can deliver fluidic cooling to microprocessors, or even to create ultra-low dielectric constant air-gaps for integrated circuits.[1–3]

Polycarbonates, such as poly(propylene-carbonate) (PPC) can be used as sacrificial polymers. Complete thermal decomposition of PPC occurs at 200–300°C; however, this decomposition can be catalyzed in the presence of strong acids that would enable low temperature decomposition. The polycarbonate decomposition process can be activated by reacting the unpaired electrons of the carbonyl oxygen with a strong acid. The acid catalyzed decomposition lowers the decomposition temperature to 100–180°C. The mechanism for the acid catalyzed processing of PPC was earlier reported by Jayachandran et al.[2] The primary volatile products of decomposition are acetone and carbon dioxide. This mechanism is catalytic because a proton is regenerated with each subsequent decomposition reaction. Acetone and carbon dioxide are volatile gases, which can slowly permeate through many dielectrics at the decomposition temperature.

A photo-activated acid generation process is desirable because the acid catalyzed decomposition of the polycarbonate can be used to pattern the film. A photo-patternable polycarbonate can be made by mixing the polymer with a photoacid generator (PAG). Upon ultraviolet (UV) irradiation, the PAG produces an acid, as shown for example in Figure 1. The decomposition mechanism for a diphenyliodonium (DPI) cation and conjugate base of a strong acid cation is shown in Figure 1. Through a combination of UV photoexcitation and heat, the cation dissociates into two radical species, both stabilized by the presence of benzyl groups. Upon reaction with residual solvent or polymer, a proton is gener-

Correspondence to: P. A. Kohl (paul.kohl@chbe.gatech.edu).

Journal of Applied Polymer Science, Vol. 105, 2655–2662 (2007)

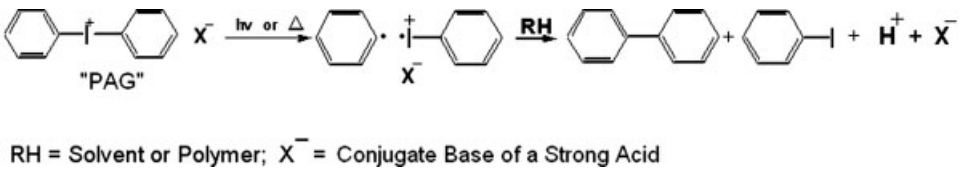

Figure 1 Mechanism for the generation of acid by the decomposition of a PAG.

ated which together with the conjugate base forms a strong acid. The reaction rates for the creation of the acid and decomposition of the polycarbonate are both a function of temperature. In addition, some acids have significantly high vapor pressures at the temperatures used leading to evaporation of the generated acid from the polymer matrix. Acids with very low vapor pressures, approaching zero, leads to concentration of the acid in the polycarbonate as the film decomposes and precipitation of the nonvolatile PAG salts when the polycarbonate leaves. Nonvolatile PAGs products[8] ultimately results in excess mass or residue remaining on the surface.

The presence of residual mass or residue remaining on the substrate after the decomposition of PPC is an important consideration because it can interfere with operation of the MEMS device or give the air-cavity undesirable properties. This residue can result from several polymer related factors in addition to the PAG. For example, the polymer may not a pure polycarbonate and may contain polyether or other impurities originating during the polymerization process. In addition, acid initiated decomposition of ethers or other impurities is a potential concern because the decomposition product can consume the acid and not regenerate it. The acid catalyzed decomposition of ether can result in the formation of an alcohol, which effectively acts as a catalyst poison.

In this study, several effects of different PAGs on the decomposition of polycarbonate are investigated. The rate of polycarbonate decomposition and resulting residue are measured as a function of acid strength, acid volatility, and ambient conditions during decomposition of the polycarbonate.

EXPERIMENTAL

The PPC (Aldrich Chemical) was dissolved in 99+% pure γ-butyrolactone (GBL) (Sigma-Aldrich). Table I is a summary of the PAGs used in this study grouped by anion moiety.[9–12] All materials were used as-received.

The PPC films were spin-coated onto 100 mm diameter, *p*-type silicon wafers (Polishing Corp of America) and soft-baked using a spin coater/hotplate tool (Brewer Science, Model #2031050). A UV exposure system (ThermoOrion Instruments) was used to activate the PAGs. A Sloan Dektak 3 surface profilometer was used to measure film thicknesses. A 30 wt % polymer solution with PAG in GBL was used to cast all the PPC films. Thin polymer films (ca.

TABLE I
PAG List

PAG chemical name	Acronym	Supplier
Triflic acid group		
(*tert*-Butoxycarbonylmethoxynaphthyl)-diphenylsulfonium triflate	TBOMDS-TF	Sigma-Aldrich
Bis(4-*tert*-butylphenyl)iodonium triflate	BTBPI-TF	Sigma-Aldrich
N-Hydroxynaphthalimide triflate	NHN-TF	Sigma-Aldrich
Nonaflic acid group		
Diphenyliodonium perfluoro-1-butanesulfonate	DPI-NF	Sigma-Aldrich
Tris(4-*tert*-butylphenyl)sulfonium perfluoro-1-butanesulfonate	TTBPS-NF	Sigma-Aldrich
N-Hydroxynaphthalimide perfluoro-1-butanesulfonate	NHN-NF	Midori Kagaku Co.
FABA acid group		
4-Methylphenyl[4-(1-methylethyl)phenyl] iodonium tetrakis (pentafluorophenyl)borate	Rhodorsil-FABA	Rhodia
Tris(4-*tert*-butylphenyl)sulfonium tetrakis-(pentafluorophenyl)borate	TTBPS-FABA	Rhodia
Triphenylsulfonium tetrakis-(pentafluorophenyl)borate	TPS-FABA	Rhodia
Sulfonate (non-fluorinated) acid group		
Bis(4-*tert*-butylphenyl)iodonium *p*-toluenesulfonate	BTBPI-PTS	Sigma-Aldrich
Diphenyliodomium 9,10-dimethoxyanthracene-2-sulfonate	DPI-DMOS	Sigma-Aldrich
Ciba non-ionic photoacid generator	CGI 263	Ciba Specialty Chemicals
Specialty acid group		
Bis(4-*tert*-butylphenyl)iodonium tris(perfluoromethanesulfonyl)methide	BTBPI-TMM	3M Corporation
Bis(4-*tert*-butylphenyl)iodonium bis(perfluorobutanesulfonyl)imide	BTBPI-BBI	3M Corporation
Bis(4-*tert*-butylphenyl)iodonium perfluoro-1-octanesulfonate	BTBPI-HDF	Midori Kagaku Co.

10 μm) were spin case at 4000 rpm for 30 s. with a ramp rate was 500 rpm/s. Medium thickness films (ca. 25 μm) were spun at 1900 rpm for 30 s. with a 300 rpm/s ramp rate. Thick films (ca. 50 μm) were spun for 30 s. at 950 rpm with a 250 rpm/s ramp rate. In all cases, the polymer was dynamically dispensed onto the substrate, while the wafer was spun at 500 rpm.

The PAG loading was 4% Rhodorsil-FABA by weight of the polymer. The same molar concentration as the Rhodorsil-FABA was used for the other PAGs. The films were soft baked in an oven at 120°C for 10, 12, or 15 min for the thin, medium, and thick films, respectively, to remove the solvent from the polymer. All UV exposures were at 248 nm and 4 J/cm^2 dose. This high dose was chosen to ensure complete activation of the PAGs.[13] The nitrogen-purged tube furnace experiments were performed at a nitrogen flow rate of 2 L/min for 30 min prior to sample heating. In the screening experiments, a 2-h decomposition was performed after exposure, unless otherwise stated. The rate of decomposition was measured by measuring the thickness of the residue after 1, 5, 10, 15, 20, 25, and 30 min. Glass slides were used as substrates for the films to examine the color of the residue. The thickness of the residue was measured at three different locations on each of two samples.

The surface chemical composition was studies by X-ray photoelectron spectroscopy (XPS), taking the integrated area under the photoelectron peak for each element weighted by their individual sensitivity factors (photoelectron emission cross section).

RESULTS AND DISCUSSION

It has previously been shown that PPC can be decomposed thermally or the decomposition can be catalyzed by a strong acid.[2,3] Figure 2 shows the thermogravimetric analysis (TGA) for the decomposition and volatilization of PPC. In the TGA, the temperature was ramped at 10°C/min and the weight loss occurred between 200 and 300°C. When tetrakis(pentafluorophenyl)borate-4-methylphenyl[4-(1-methylethyl)-phenyl]iodonium (Rhodorsil-FABA) was used as a PAG and mixed with the PPC and irradiated with 800 mJ/cm^2 of energy (248 nm wavelength) the acid catalyzed decomposition of PPC occurred. The onset weight loss of the irradiated PAG-Polymer film started about 100°C. When the UV irradiation is omitted for the PAG loaded polymer, the PAG undergoes thermal activation and begins to decompose the polymer at 150°C. These temperature differences allow a PPC/PAG film to be patterned by typical lithography methods. Figure 2 also provides the guidelines for altering the PPC decomposition temperature around parameters set by the system. The

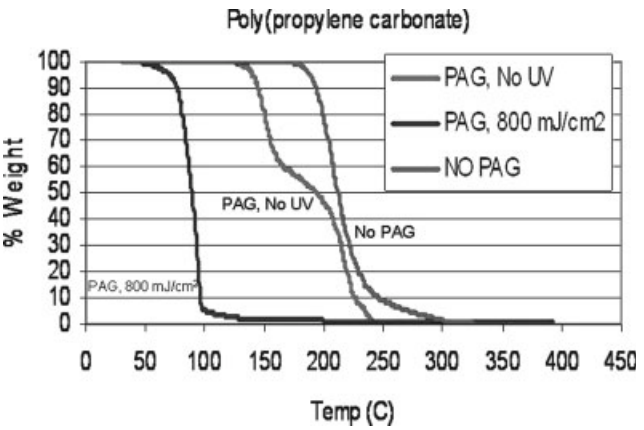

Figure 2 Sample TGA for a photoactive PPC system with a temperature ramp rate of 10°C/min.

ability of other PAGs to activate and decompose PPC is of interest, thus, a number of PAGs were surveyed.

PAG survey

The fraction of the PPC film decomposed after irradiation at 4 J/cm^2 dose (248 nm) and baking at 60, 90, or 120°C for 2 h on a hot plate or in a nitrogen-purged oven was evaluated. These are conditions potentially favorable for photoactivating the PAG and acid catalyzing the decomposition of the PPC. Table II shows the percentage of a 10-μm thick polymer film spin-coated onto a silicon wafer remaining after the baking step when compared with the thickness of the film present prior to baking. Table II is arranged according to acid type. Within each group many of the results are similar with the exception of the perfluorosulfonyl imides and methides. Within each acid group, the cation (nonacid part of the PAG) is varied, which generally has a minor effect on the efficiency of the PAG. The cation can affect the UV absorbance of the PAG, solubility in solution, and thermal stability. The UV absorbance should not be a factor here since the UV dose is very high. There is however a large difference in percent decomposition between acid groups. The properties of the acid, such as acid strength, vapor pressure, and solubility have a dramatic effect on the catalytic performance of the PAG. The sulfonate group has poor efficiency over the entire range of experiments. The poor results are likely due to the lower acidity of the nonperfluorinated acids generated by this group of PAGs. Each acid in this group has a pKa of ~ -4, which does not place them in the superacid category.[14] It has been shown in previous studies that PPC is effectively decomposed by acids with a pKa of -12 and below (superacid range).[14]

The triflic acid group in Table II shows greater decomposition than the nonperfluorinated sulfonic

TABLE II
PPC Film Decomposition Percentages for Each Processing Condition and PAG

	Nitrogen furnace			Open air hotplate		
PAG	60°C	90°C	120°C	60°C	90°C	120°C
Triflic acid group						
TBOMDS-TF	15%	27%	24%	0%	7%	11%
BTBPI-TF	13%	20%	20%	1%	4%	6%
NHN-TF	7%	16%	19%	3%	9%	6%
Nonaflic acid group						
DPI-NF	8%	31%	34%	5%	22%	27%
TTBPS-NF	17%	29%	33%	0%	13%	22%
NHN-NF	9%	34%	32%	6%	14%	23%
FABA acid group						
DPI-FABA	51%	98%	99%	19%	99%	98%
TTBPS-FABA	6%	89%	94%	2%	85%	91%
TPS-FABA	30%	88%	97%	63%	94%	96%
Perfluorosulfonyl imides and methides						
BTBPI-TMM	27%	96%	98%	4%	97%	97%
BTBPI-BBI	22%	17%	15%	21%	12%	10%
BTBPI-HDF	26%	40%	38%	21%	29%	39%
Sulfonate acid group						
BTBPI-PTS	4%	2%	5%	2%	1%	10%
DPI-DMOS	13%	7%	6%	3%	2%	7%
CGI 263	8%	11%	10%	4%	0%	11%

acid group. With a pKa measured at ~ -14, triflic acid has the adequate acidity to catalyze the decomposition of PPC.[14] However, the vapor pressure of triflic acid is high at these temperatures (50–175 Torr).[9] Since there is a large surface to volume ratio in these thin, 10-μm films, the high vapor pressure results in acid evaporation and thus lower acid concentration in the film. If the vapor pressure is too high, the acid evaporates before complete decomposition of the PPC. The rate of acid evaporation from the film will be discussed later in this section. To support the argument that it is the volatility of the triflic acid, which lowers the overall PPC decomposition, experiments were preformed with PAGs containing acid, nonaflic acid, as shown in Table II. Nonaflic acid has a similar chemical structure and acidity to triflic acid except for a longer perfluorinated carbon chain (four carbons compared with one carbon). The vapor pressure of nonaflic acid is 10–40 Torr at the temperatures used here, which is significantly lower than triflic acid.[9,14] The fractional decomposition of PPC with nonaflic acid PAG is more than 50% greater than the result with triflic acid PAGs most likely due to its lower vapor pressure.

The effect of vapor pressure was considered in experiments with bis(4-*tert*-butylphenyl)iodonium perfluoro-1-octanesulfonate (BTBPI-HDF). With an eight carbon chain, the acid formed also had a lower vapor pressure than triflic acid at the temperatures used (1–10 Torr), while the acid strength was similar to triflic acid.[9] The maximum decomposition with the perfluoro-octanesulfonate was 38% (furnace heating at 120°C) compared with 34% with nonaflic acid PAG. Thus, the PPC decomposition with perfluoro-octanesulfonate acid was close to nonaflic acids and greater than triflic acid. The BTBPI-HDF PAG had low solubility in the PPC polymer matrix, which could have negatively effected its catalytic activity. After the softbake step, phase separation was observed within the PPC film loaded with BTBPI-HDF. The phase separation, caused by the long perfluorinated carbon chain, resulted in limited mixing between the PPC and PAG and retarded the performance.

Perfluorinated imide and methide sulfonic acid PAGs were also examined, as shown in Table II. Very high decomposition levels, $\sim$ 98%, were achieved. Previous studies have shown that these PAGs are very effective at PPC decomposition.[9] The vapor pressure of the acid resulting from BTBPI-TMM is 60–65 Torr at 120°C, which is slightly higher than nonaflic acid,[9] however, its reactivity with PPC is high enough to compensate for the evaporation. The perfluorinated imide PAG, BTBPI-BBI, showed poor performance even though it has a low vapor pressure, 10 Torr at 120°C and high acidity.[9] However, phase segregation of the PAG from the PPC matrix hindered the BTBPI-BBI reaction with PPC.

The final group of PAGs tested contained FABA acids, which have been used previously.[1–3] All of the FABA acids resulted in very significant PPC film decomposition. The high efficiency is attributed to the extreme acidity, low vapor pressure of the acid, and high solubility of the PAG in PPC film. The low vapor pressure of the acid is due to the bulky anion. Although the FABA-based PAGs were highly efficient at catalyzing decomposition of PPC, a small residue remained. Analysis of these residues is reported later in this section.

Effect of ambient atmosphere on PPC decomposition

The effect of the ambient during PPC decomposition is shown in Table II. Two different heating methods have been used: a hotplate exposed to room air and a nitrogen purged tube oven. Several of the PAG/PPC samples, most notably the triflic and nonaflic acid based PAGs; the open-atmosphere hotplate samples had a lower efficiency for PPC decomposition than the nitrogen-purged tube furnace. There several differences between the open-aired hotplate and nitrogen-purged furnace. The oxygen, moisture and other gases in air can effect the decomposition of the PPC, The heating rate of the temperature on a hotplate is much faster than in a convectively heated oven. It is possible that the time spent at lower temperatures during convective heating in an oven has a different PPC decomposition efficiency than at higher temperatures. This is especially true for PAGs where there is competition between evaporation of the acid and ca-

talysis of the PPC. Finally, the hotplate heats the films from the inside-out compared with a convectively heated oven, which heats the outside of the film first.

Water vapor is an important parameter in the acid creation and thermal decomposition process. Burns et al. examined the effect of humidity on the deprotection kinetics of several photoresists.[15] Photoresists are dependent on an acid catalyzed deprotection reaction. The presence of water vapor in the atmosphere serves to hinder the overall performance of the resist. The presence of water lowers the acid strength within the chemically amplified photoresist because the strongest acid present is the hydronium ion, not the superacid.[15] Similar effects can occur within the acid-catalyzed PPC films. The effect of water on the acid catalyzed process was investigated by performing the PPC decomposition in a dry and humidified and nitrogen filled tube furnace. Table III shows the percentage of the PPC decomposed as a function of relative humidity (0, 33, 66, and 100%) within the nitrogen filled tube oven. The relative humidity reported in Table III is based on the humidity at 20°C, not at the elevated temperature during decomposition. The triflic and nonaflic acids showed a 40% decrease in PPC decomposition for the saturated humidity versus dry conditions, consistent with a pH-leveling effect. Conversely, the perfluorinated methide and FABA PAGs did not show a significant decrease in efficiency with humidity. The high reactivity and hydrophobic nature of the perfluoro-compounds is likely responsible for the insensitivity of the two PAGs, as discussed later in this section.

The effect of temperature ramping was investigated to see if time spent at lower temperatures had a significant impact on the efficiency of the decomposition. The surface of the hotplate was heated from ambient conditions to the desired set-point of 120°C at a gradual rate, 3–5°C/min, similar to the rate of heating in a tube oven. The comparison between rapid hotplate heating and gradual heating for the triflic and nonflic acid PAGs are shown in Table III. No statistical difference was found between the two heating conditions.

Hotplate decomposition performance versus substrate type was also examined for the trilfic and nonaflic acid PAGs. The substrates chosen were silicon and glass. During hotplate PEB processing, the higher thermal conductivity of silicon relative to glass allows a higher heat flux to the PPC film. For highly volatile acids, like triflate and nonaflate, the higher heat flux should help to counteract the time restraints placed on the system by the rapid evaporation of the acid, thus improving decomposition. The results for hotplate processing at 120°C with DPI-NF showed an increase in overall decomposition efficiency from 27% with a glass substrate to 33% on a silicon substrate. Similarly, results with TBOMDS-TF showed an increase in the decomposition from 11% with glass to 15% with silicon.

Differential rate of decomposition

The instantaneous rate of decomposition was not constant with time. A rapid rate will likely lead to higher pattern fidelity since diffusion of the photogenerated acid is minimized. Cleavage of a single carbonate linkage does not lead to weight loss since small molecular weight products are needed for vaporization. The polymer decomposition can be represented by an Arrhenius model, eq. (1).

$$\frac{d\alpha}{dt} = k(1-\alpha)^n = A\ \exp\left(-\frac{E_a}{RT}\right)(1-\alpha)^n \qquad (1)$$

where α is a dimensionless mass fraction, k is the rate constant, n is the reaction order, A is the Arrhenius pre-exponential factor, E_a is the activation energy, R is the universal gas constant, t is the time, and T is the temperature.[16] Wu et al. used a constant reaction rate versus mass fraction, which is reasonable for their specific polymer decomposition process.[16] However, significant deviation from ideal fitting may occur in the carbonate cleavage process because the polymer contains a small amount of an impurity, which can consume the acid. Also, evaporation of the photogenerated acid changes the concentration of the acid within the film. The film thickness was measured as a function of time by making multiple samples and measuring each at a different time in the decomposition process. Figure 3 shows

TABLE III
Effect of Humidity on the Percentage PPC Decomposition for Various PAGs

	Percentage decomposition					
PAG	0% Wet nitrogen	33% Wet nitrogen	66% Wet nitrogen	100% Wet nitrogen	Rapid hotplate heating	Gradual hotplate heating
BTBPI-TF	19.2%	13.7%	13.6%	11.5%	10.5%	11.1%
DPI-NF	34.5%	30.6%	28.4%	20.9%	25.1%	24.5%
BTBPI-TMM	97.9%	–	–	98.4%	97.2%	–
Rhodorsil-FABA	99.4%	–	–	95.6%	98.5%	–

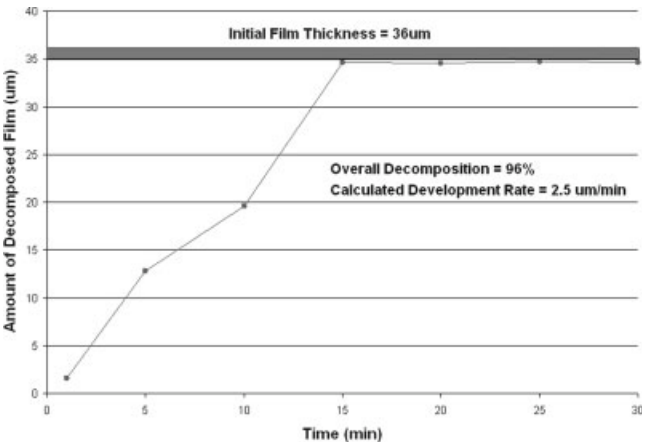

Figure 3 Rate of decomposition plot for Rhodorsil-FABA at 120°C hotplate PEB with a 36 μm initial film thickness.

the PPC thickness versus time for the Rhodorsil-FABA PAG in PPC. The decomposition rates for several PAGs are shown in Table IV. The rates were calculated using linear regression averaged over the time ranges. Figure 3 shows that the decomposition process is complete after about 15 min and the rate of decomposition is constant at 2.5 μm/min. The rate of PPC decomposition varies from PAG to PAG. The highest rate was for BTBPI-TMM, which is consistent with the reactivity results by Lamanna et al.[9] The rapid rate of decomposition is important because of the high vapor pressure of BTBPI-TMM. If the acid does not catalyze PPC decomposition before evaporation of the acid, then the undecomposed polymer would remain on the surface as residue.

The high rate of acid evaporation, such as with DPI-NF, results in a lower reaction rate. This effect can be seen by comparing the decomposition rate for different polymer thicknesses. Decomposition of a 10 μm DPI-NF PPC results in 34% decomposition. Decomposition of a thicker, 25-μm film, resulted in 63% decomposition, and a 44-μm film resulted in 86% decomposition. The greater fractional decomposition was because the acid remained in the thicker film longer (greater volume for the same surface area). Evaporation of the acid occurs at the surface whereas decomposition occurs throughout the film. Diffusion of the acid through the film to the surface can be modeled by one-dimensional diffusion, eq. (2).

$$D\frac{\partial^2 C}{\partial z^2} = \frac{\partial C}{\partial t} \tag{2}$$

where D is the diffusion coefficient for the acid in PPC, C is the concentration of the acid, z is the axis of diffusion, and t is the time. The reaction term is ignored through the bulk of the film because ideally, the acid is not consumed in the catalytic reaction. The initial condition is that the concentration of acid in the PPC, C^0, at time zero is uniform with thickness. The two boundary conditions used are that the flux of acid at the polymer–glass interface is zero and the concentration of acid at the PPC surface is zero. A linear gradient in concentration is assumed in the depletion region, eq. (3).

$$-D\frac{dc}{dz} = k_c(C^g - C^{\inf}) \quad \text{for all } t > 0, \text{at } z = l \tag{3}$$

where k_c is the mass transfer coefficient, C^g is the concentration of the acid on the surface of the film in the gaseous state, $C^{\inf}$ is the concentration of the gas at the edge of the boundary layer and the surrounding gas, and l is equal to the thickness of the film. The relationship between the surface of the film and the gas is given by eq. (4).

$$C^s = KC^g \tag{4}$$

where C^s is the concentration of the acid on the surface of the film in the solid and K is the partition coefficient between the two phases yielding eq. (5).

$$\frac{dc}{dz} = -\left(\frac{k_c}{DK}\right)C^s \quad \text{for all } t > 0, \text{ at } z = l \tag{5}$$

If the mass transfer in the system is fast, the equation becomes diffusion limited.

Stewart et al. evaluated the diffusion coefficient in poly(4-isopropyloxycarbonyloxystyrene) (IPOCST) and poly(4-neopentyloxycarbonyloxystyrene) (NPOCST). The diffusion coefficient in PPC is similar to that in IPOCST and NPOCST when heated to their individ-

TABLE IV
Complete Rate of Decomposition Data Set at 120°C Hotplate PEB

PAG	Initial film thickness (μm)	Overall decomposition percentage	Completed decomposition time (min)	Calculated development rate (μm/min)
TBOMDS-TF	42.5	15	25	0.93
DPI-NF	44.0	86	25	1.5
BTBPI-TMM	47.0	99	10	4.5
Rhodorsil-FABA	36.0	96	15	2.5

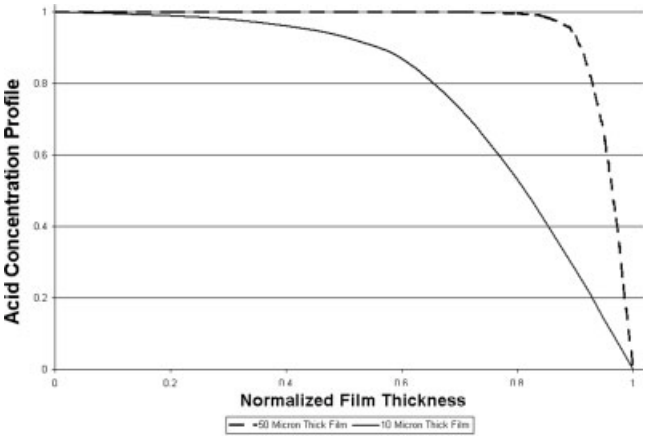

Figure 4 Graphical PDE solution for 10 and 50-μm films using an estimated diffusion coefficient for DPI-NF over 30 min.

ual T_g's. The T_g's of IPOCST and NPOCST are 88 and 82°C, respectively,[17] The T_g of PPC is 40°C resulting in a diffusion coefficient of 1.89×10^{-11} cm^2/s. Figure 4 shows the acid concentration profile in a 10 and 50-μm thick films after 30 min at 120°C. This shows that the total acid content in the 50-μm thick film after 30 min is significantly higher than in the 10-μm thick film. Thus, the percent decomposition of the 50-μm thick film with DPI-NF PAG is substantially higher than the 10-μm thick film.

Combination PAG film

Although the FABA acid has very high decomposition rate and little residue, it's near-zero vapor pressure is partly responsible for some of the residue that remains on the surface of the silicon. More volatile PAGs, such as DPI-NF, appear to leave residue because some of the acid evaporates from the system leaving an inadequate acid concentration at the end of the decomposition process. The two PAGs, Rhodorsil-FABA to DPI-NF, were both added to the PPC; however, their concentrations were below the amount needed individually for decomposition of the PPC. The intention is that as the DPI-NF evaporates during PPC decomposition, the concentration of Rhodorsil-FABA is increases due to film shrinkage. The combined PAG loading was 3% molecular weight equivalent DPI-NF and 1% molecular equivalent Rhodorsil-FABA. The percent decomposition of the PPC with the mixture of PAGs is 98%, whereas the decomposition with only DPI-NF was 33–86% (thickness dependent). The PPC decomposition with 1% Rhodorsil-FABA was 8%. Furthermore, the combined PAG loading showed the same percent decomposition over a wide range of film thicknesses from 10 to 50 μm. For a 45-μm film, the rate of decomposition was calculated to be 2.5 μm/min.

Residue analysis

The composition and origin of the residue remaining on the surface of the substrate is of interest. XPS was used to identify the chemical state of the residue. The elemental composition is shown in Table V. The Rhodorsil-FABA residue was 30.6% fluorine. This fluorine percentage is considerably greater than in the initial Rhodorsil-FABA PPC mixture. This fluorine enrichment shows that the PAG is the major contributor to the residue. The boron content was found to be 1.5%, and the iodine contribution was 0.2%. The result is stoichiometrically correct since there are 20 fluorine atoms per boron in the PAG. Given that the residue contained 7.5 times more boron than iodine, the acid formed from the activation of the anion (not the cation) is a major contributor to the residue. The oxygen content in the residue originates from the PPC or product from reaction with air. The oxygen content was found to be 2.3% of the residue. Since the main source of oxygen is the polymer, the low percentage of oxygen combined with the high percentage of fluorine suggests that there is little polycarbonate remaining on the substrate after PEB. Since the polymer, PAG, and solvent contain carbon, no unique conclusions drawn from the carbon data.

The BTBPI-TMM PAG has nine fluorine atoms per ion and the residue had 8.9% fluorine. The low fluorine content is consistent with the vapor pressure of the acid for the methide acid. In addition, the XPS data shows that there is 3.2% sulfur in the residue. This value is approximately one third the amount of fluorine, which is stiochiometrically correct. Finally, the second most abundant element in the BTBPI-TMM residue is oxygen with a concentration of 11.3%. This result is not as definitive as with the FABA PAG since there are oxygen contributions from both the PAG anion and PPC.

The Combination PAG XPS data shows that the fluorine abundance was 10.7%. This lower salt residue is due to the use of the volatile triflate PAG. The oxygen contribution for this residue was found to be 16.4%. The carbon content was higher than either the BTBPI-TMM and Rhodorsil-FABA PAG samples. Since there is no oxygen contribution from the FABA acid and only 3 atoms of oxygen per molecule of nonaflic acid, the majority of this oxygen was a product of

TABLE V
Summary of XPS Elemental Abundance Data for PPC/PAG Residues After Post Exposure Bake

	XPS calculated elemental abundance (%)					
PAG	C	O	F	S	B	I
Rhodorsil-FABA	65.4%	2.3%	30.6%	–	1.5%	0.2%
BTBPI-TMM	76.6%	11.3%	8.9%	3.2%	–	–
Combination PAG	72.9%	16.4%	10.7%	–	–	–

TABLE VI
Summary of XPS Carbon Bonding Data for PPC/PAG Residues After Post Exposure Bake

	XPS calculated carbon bonding data (%)					
PAG	C—C	C—O	C—S	C—F	$C—F_2$	$C—F_3$
Rhodorsil-FABA	62.0%	7.6%	–	30.3%	–	–
BTBPI-TMM	84.6%	5.7%	5.4%	–	–	4.2%
Combination PAG	68.3%	17.7%	–	11.1%	2.8%	–

unreacted polymer. The residue appeared colorless and transparent like the original PPC film. This was different from the higher FABA-based residues. Moreover, the XPS analysis produced no measurable presence of boron, sulfur, or iodine, which were in the starting PPC films. These results support the conclusion that the majority of the residue is composed of unreacted polycarbonate and not PAG.

Data on the oxidation state of some of the elements is shown in Table VI. The carbon bonding data for each of the PAGs was examined. The Rhodorsil-FABA data in Table VI shows that 30.2% of the carbon bonding was to a fluorine. This high percentage of carbon–fluorine bonds can only be from the FABA PAG portion of the PAG/PPC mixture. Further, the chemical shift is consistent with carbon atom being bonded to a single fluorine atom, as in the FABA acid. The carbon–oxygen contribution was low, suggesting that unreacted PPC comprise a small fraction of the residue. The BTBPI-TMM PAG showed a low percentage of carbon–fluorine bonding, 4.2%. This data supports the conclusion that most of the methide acid has evaporated from the system completion of the decomposition process. Furthermore, the CF_3 bonds that were identified in the XPS matches the chemical structure of the acid. The carbon bonding data in the combination PAG residue showed results that support high PAG evaporation concept. The data shows that 11.1% of the carbon–fluorine bonds were CF single bonds and only 2.8% of the carbon fluorine bonds were CF_2. Since CF bonding groups are an indication of the FABA acid and CF_2 bonding groups are from the nonaflic acid, there is approximately four times more FABA acid than nonaflic acid in the residue. The combination acid contained three times more nonaflic acid than FABA acid. This finding demonstrates that the more volatile acid has evaporate, while the bulky FABA acid remained in the film to complete the decomposition. Additionally, the large percentage of carbon–oxygen bonding confirms that the residue is primarily polymer and not the PAG.

CONCLUSIONS

The catalyzed decomposition of PPC was studied as a function of photoacid type. The two acids were found to decompose >98% of the PPC: Rhodorsil-FABA and BTBPI_TMM. Triflic acids, nonaflic acids, perfluorooctane sulfonic acids, and nonperfluorinated sulfonic acids decomposed only a portion of the films. The affect of water vapor on the decomposition of PPC was examined and found to be PAG dependent. Acids with lower reactivity were affected more by water. A combination of two PAGs with different vapor pressures, Rhodorsil-FABA and DPI-NF resulted in 98% decomposition. XPS was used to analyze the chemical bonding and composition of the residue left on the substrates after the PEB of the PPC film. The bulk of the residue from the Rhodorsil-FABA PAG PPC samples was caused by the acid. Whereas, the majority of the residue left behind by the BTBPI-TMM PAG was due to low molecular weight, partially unreacted polymer.

References

1. Joseph, P. J.; Kelleher, H. A.; Allen, S. A. B.; Kohl, P. A. J Micromech Microeng 2005, 15, 35.
2. Jayachandran, J. P.; Reed, H. A.; Zhen, H.; Rhodes, L. F.; Henderson, C. L.; Allen, S. A. B.; Kohl, P. A. J Microelectromech Syst 2003, 12, 147.
3. Reed, H. A.; White, C. E.; Rao, V.; Allen, S. A. B.; Henderson, C. L.; Kohl, P. A. J Micromech Microeng 2001, 11, 733.
4. White, C. E.; Henderson, C. L. Adv Resist Technol Process XXI 2004, 5376, 850.
5. White, C. E.; Henderson, C. L. Adv Resist Technol Process XIX 2002, 4690, 242.
6. Joseph, P.; Pejman, M.; Ayazi, F.; Kohl, P. A. IEEE Trans Adv Packag, to appear.
7. Monajemi, P.; Joseph, P. J.; Kohl, P. A.; Ayazi, F. J Micromech Microeng 2006, 16, 742.
8. Salas, J.; Joseph, P. J.; Kelleher, H. A.; Park, S.; Allen, S. A. B.; Kohl, P. A. J Vacuum Sci Technol B 2004, 22, 953.
9. Lamanna, W. M.; Kessel, C. R.; Savu, P. M.; Cheburkov, Y.; Brinduse, S.; Kestner, T. A.; Lillquist, G. J.; Parent, M. J.; Moorhouse, K. S.; Zhang, Y.; Birznieks, G.; Kruger, T.; Pallazzotto, M. C. Adv Resist Technol Process XIX 2002, 4690, 817.
10. Ciba Specialty Chemicals. Photoacid Generators for Microlithography. (January 2003). Retrieved June 2005, from http://www.cibasc.com/rz_photoacid_generators1.pdf
11. Sigma-Aldrich. Electronic Catalog on Photoacid Generators. Retrieved March2005, Sigma-Aldrich United States Web Site: http://www.sigmaaldrich.com/Area_of_Interest/The_Americas/United_States.htm
12. Midori Kagaku Co., Ltd. Electronic Catalog on Photoacid Generators. Retrieved May 2005, Midori Kagaku Co. English Web Site: http://www.midori-kagaku.co.jp/m000908/e_index.htm
13. Fedynyshyn, T. H.; Sinta, R. F.; Mowers, W. A.; Cabral, A. Adv Resist Technol Process XX 2003, 5039, 310.
14. Rhodia global solutions for acid catalytic systems. (n.d). Retrieved November 2005, from http://www.rhodia-ppa.com/media/PPA/push/Product/Acilys/acilysbrochure_final.pdf
15. Burns, S. D.; Medeiros, D. R.; Johnson, H. F.; Wallraff, G. M.; Hinsberg, W. D.; Willison, C. G. Adv Resist Technol Process XIX 2002, 4690, 321.
16. Wu, X.; Reed, H. A.; Wang, Y.; Rhodes, L. F.; Elce, E.; Ravikiran, R.; Shick, R. A.; Henderson, C. L.; Allen, S. A. B.; Kohl, P. A. J Electrochem Soc 2003, 150, H205.
17. Stewart, M. D.; Becker, D. J.; Stachowiak, T. B.; Schmid, G. M.; Michaelson, T. B.; Tran, H. V.; Willison, C. G. Adv Resist Technol Process XIX 2002, 4690, 943.